

# Low-field anomalous magnetic phase in the kagomé-lattice shandite $\text{Co}_3\text{Sn}_2\text{S}_2$

Mohamed A. Kassem<sup>\*,†</sup>, Yoshikazu Tabata, Takeshi Waki, Hiroyuki Nakamura

Department of Materials Science and Engineering, Kyoto University, Kyoto 606-8501, Japan.

## Abstract

The magnetization process of single crystals of the metallic kagomé ferromagnet  $\text{Co}_3\text{Sn}_2\text{S}_2$  was carefully measured via magnetization and AC susceptibility. Field-dependent anomalous transitions in the magnetization indicate a low-field unconventionally ordered phase stabilized just below  $T_C$ . The magnetic phase diagrams in applied fields along different crystallographic directions were determined. The magnetic relaxation process studied in frequencies covering five orders of magnitude from 0.01 to 1000 Hz indicates characteristic relaxation times of several seconds at the borders of the anomalous phase. Our results arise a lot of questions about the nature of  $\text{Co}_3\text{Sn}_2\text{S}_2$  magnetic states.

## 1. Introduction

The kagome-lattice, a 2-dimensinal (2D) conner-sharing triangular-lattice, is a platform of many exotic phenomena originated from its geometry. For instance, antiferromagnetic-coupled spin system on the kagomé-lattice is highly-frustrated and can exhibit quantum disordered spin liquid<sup>1</sup> and exotic magnetic ordered states with non-trivial spin textures<sup>2-5</sup>. The geometric spin frustration is one of the most intriguing issues in recent condensed matter physics<sup>6-9</sup>. The asymmetric Dzaloshinski-Moriya (DM) interaction is another driving force of non-trivial spin textures in the kagomé-lattice magnets<sup>8-11</sup>. The DM interaction can destabilize collinear ferro- and antiferromagnetic orders and results in spiral and canted spin structures. Furthermore, a topologically-protected vortex-like spin texture, called as "skyrmion", is also induced by the DM interaction. Theoretically, spontaneous triangular-lattice formation of skyrimons was proposed in the presence of the DM interaction based on the phenomenological continuum model<sup>12</sup>. Indeed, the skyrmion-lattice phase was experimentally observed in noncentrosymmetric chiral<sup>13-17</sup> and polar<sup>18</sup> crystals under finite field and in the vicinity of  $T_C$ .

$\text{Co}_3\text{Sn}_2\text{S}_2$  consists of Co-Sn metallic layers, stacked along  $c$ -axis in the hexagonal setting of  $R\bar{3}m$  structure, that are separated by Sn-S blocks<sup>19-24</sup>. In each layer, Co atoms are arranged in a 2D-kagomé sublattice as shown in Fig. 1. Previously reported

studies of the magnetization process of the halfmetallic ferromagnet  $\text{Co}_3\text{Sn}_2\text{S}_2$ <sup>24,25</sup> have explored high axial anisotropy in magnetization  $M(T, H)$ <sup>26,27</sup>. The Curie temperature,  $T_C$ , and the spontaneous moment at 2 K in the easy  $c$ -axis were reported as 174 K and  $\sim 0.3 \mu_B/\text{Co}$ , respectively. Recent comprehensive magnetization measurement and analysis based on the spin fluctuation theory revealed the quasi-two-dimensionality (Q2D) of the magnetism in  $\text{Co}_3\text{Sn}_2\text{S}_2$  and its In-substituted system<sup>28</sup>. This implies that  $\text{Co}_3\text{Sn}_2\text{S}_2$  is a model system of the 2D kagomé-lattice ferromagnet and has a potential to exhibit exotic magnetic states with nontrivial spin textures.

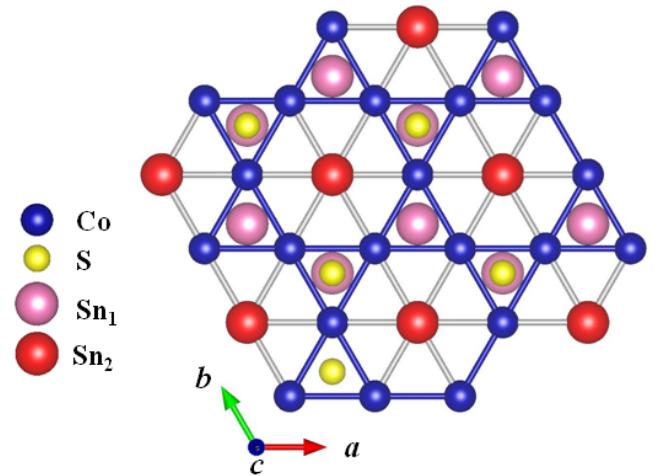


**Figure 1:** Crystal structure projection in (001)-plane showing a Co-kagomé sublattice in  $\text{Co}_3\text{Sn}_2\text{S}_2$ .

In this paper, we present results of magnetization,  $M(T, H)$ , and AC susceptibility,  $\chi_{ac}(T, H)$ , of  $\text{Co}_3\text{Sn}_2\text{S}_2$  systematically accumulated at low-fields and clearly indicate low-field anomalous magnetic phase just below  $T_C$ . The anomalous phase shows slow dynamics indicating a frozen magnetic state with characteristic relaxation times longer than 10 sec.

## 2. Experimental Details

Single crystals of  $\text{Co}_3\text{Sn}_2\text{S}_2$  used in this work have been grown by a flux method<sup>29,30</sup>. Magnetization processes were measured using a SQUID magnetometer (MPMS, Quantum Design) with magnetic fields applied parallel and perpendicular to the easy  $c$ -axis. For the AC susceptibility measurements, 1 Oe drive AC field of different frequencies was superimposed on the bias field and both were applied along the  $c$ -direction. Two experimental regimes have been followed in the measurement of temperature-scans: (i) Zero-field-cooled (ZFC) scans, after resetting the magnetometer to zero field, the sample was brought to 5 K under zero field. The magnetic fields were applied at 5 K and the measurement were performed by increasing stepwise the temperature, after thermal equilibrium was reached at each temperature. (ii) Field-cooled (FC) scans, in which the sample was cooled from 250 K, where the DC and/or AC magnetic fields were applied, and the measurement was performed with decreasing stepwise the temperature. At each temperature the sample was brought to thermal equilibrium before the measurement.

The spin relaxation processes at selected temperatures were systematically studied by measuring the ZFC AC susceptibility for different magnetic fields in a frequency range of five orders of magnitude from 0.01 to 1000 Hz. For the frequency scans, the above ZFC regime was followed and the fields were applied at the temperature of interest before the measurement.

## 3. Results

### 3.1. Magnetization

The temperature dependences of the ZFC and FC magnetizations  $M(T, H)$  of  $\text{Co}_3\text{Sn}_2\text{S}_2$  single crystal measured at various low magnetic fields

applied along and perpendicular to the  $c$ -axis are shown in Figs. 2(a) and (b). Both axial and in-plane magnetizations,  $M_c$  and  $M_{ab}$ , show sharp increases at  $T_C \sim 173$  K, which correspond to the previously reported ferromagnetic phase transitions<sup>24,26,27,29</sup>. As in literature, strong magnetic anisotropy below  $T_C$  was confirmed below  $T_C$ . The difference is reduced with increasing of magnetic field and disappears above  $\sim 1$  k Oe in the axial magnetization.

Interestingly, peculiar anomalies were found at low field where the ZFC and FC magnetizations separate from each other. The axial magnetization,  $M_c(T, H)$  in the FC process shows a hump-anomaly at temperature  $T_A \sim 126$  K with applying  $H = 5$  Oe, indicating another magnetic transition apart from the transition at  $T_C$ . The anomaly-temperature,  $T_A$ , slightly increases with the increasing of  $H$ . On the other hand, the ZFC magnetization shows a dip-like anomaly in the intermediate temperature range between  $T_A$  and  $T_C$ . Both the hump-anomalies in FC

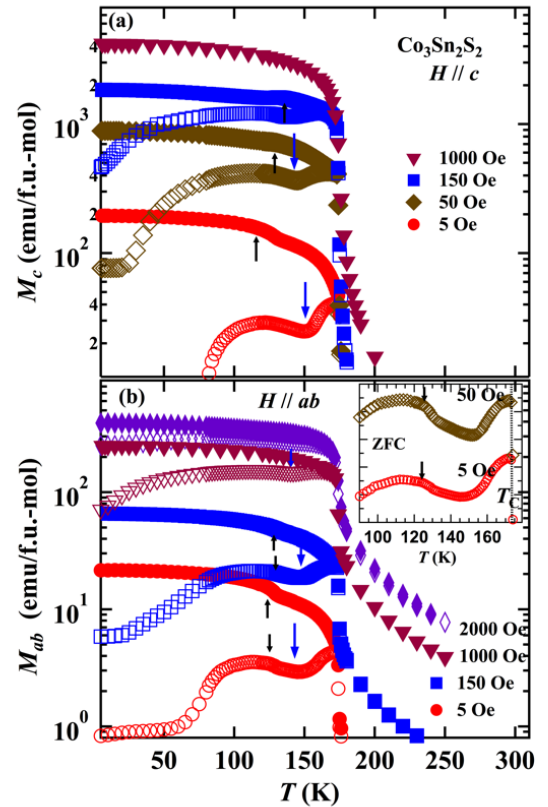


**Figure 2:** The temperature dependences of ZFC and FC magnetizations,  $M(T, H)$ , of  $\text{Co}_3\text{Sn}_2\text{S}_2$  measured at the indicated low magnetic fields applied (a) along and (b) perpendicular to the  $c$ -axis. The vertical arrows indicate the transition temperature  $T_A$  and the broad minimum (see text). The inset of (b) shows a magnification of the ZFC  $M(T)$  measured at very low fields.

$M_c(T, H)$  and the minimum in the ZFC  $M_c(T, H)$  disappear at  $H \geq 400$  Oe. One can note that the anomalies are observed at fields below the saturation fields of  $\text{Co}_3\text{Sn}_2\text{S}_2$ <sup>28</sup>.

The in-plane magnetization,  $M_{ab}(T, H)$ , displayed in Fig. 2(b), shows similar hump-anomaly at  $T_A$  in the FC process and dip-like anomaly between  $T_A$  and  $T_C$  in the ZFC process. Additionally, the ZFC  $M_{ab}(T, H)$ , also shows a hump-like anomaly at  $T_A$  at very low fields (below 150 Oe), as seen in the inset of Fig. 2(b). The field-dependences of the peculiar anomalies in  $M_{ab}$  are more gentle than those in  $M_c$ . Especially, the dip-like anomaly in the ZFC process is still observable above 400 Oe.

### 3.2. AC susceptibility of $\text{Co}_3\text{Sn}_2\text{S}_2$

For more detailed investigation of the magnetic transitions observed just below  $T_C$ , we have carefully measured the temperature-, field- and frequency-dependences of the AC susceptibility,  $\chi_{ac}$ , after ZFC and FC in a wide range of frequencies  $f$  from 0.01 to 1000 Hz. Figure 3 shows the temperature dependence of the ZFC in-phase AC susceptibility,  $\chi'(T)$ , measured with a frequency of 1 Hz and  $H=150$  Oe applied along the  $c$ -axis. For comparison, the ZFC magnetization  $M_c(T)$  measured at the same conditions is shown.  $\chi'$  shows distinct anomalies as well as observed in the dc magnetization: a sharp peak at  $T_C$ , hump-like anomaly at  $T_A$  and a broad minimum between  $T_A$  and  $T_C$ .

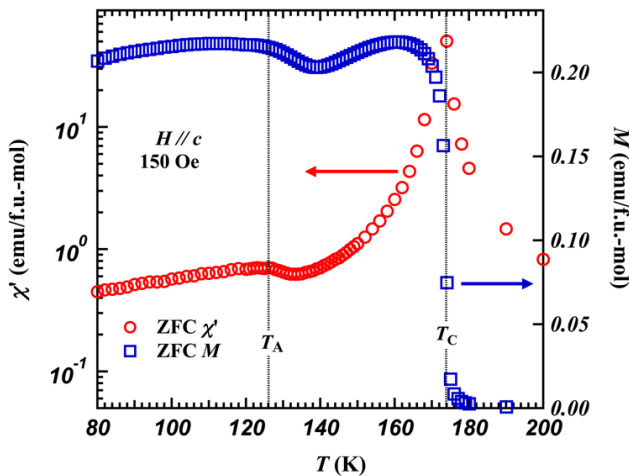


**Figure 3:** Temperature dependences of ZFC  $\chi'$  (at  $f=1$  Hz, on left axis) and  $M$  (on right axis) of  $\text{Co}_3\text{Sn}_2\text{S}_2$  at 150 Oe applied along the  $c$ -axis. The vertical dotted lines indicate  $T_A$  (see text) and  $T_C$ .

Figure 4 shows the temperature dependences of the ZFC and FC real and imaginary parts of the AC susceptibility,  $\chi'(T, H)$  and  $\chi''(T, H)$ , with  $f=1, 10, 100$  and 1000 Hz under several DC fields applied along the  $c$ -axis. The characteristic features in  $\chi'$  with  $f=1$  Hz at 150 Oe, found in Fig. 3, are recognized for all frequencies at low field (0 and 150 Oe), as shown in Figs. 4 (a) and (c). At 600 Oe, shown in Fig. 4 (e), only the anomaly at  $T_C$  is found. Absence of the hump-like anomaly and broad minimum is also recognized in the dc magnetization at higher than 400 Oe. The anomaly at  $T_C$  at 600 Oe is rather broaden, which suggests a difference of the natures at low and high fields. It should be noted  $\chi'$  in the ZFC and FC processes almost coincide each other at low and high fields, unlike the dc magnetization.

The characteristics at low field are more pronounced in the imaginary part of the ac susceptibility,  $\chi''$ , as shown in Figs. 4 (b) and (d).  $\chi''$  is almost absent above  $T_C$  and shows more rapid increasing at  $T_C$  than  $\chi'$ . The anomalies below  $T_C$  in  $\chi''$  are not so distinct as in  $\chi'$ , except for that with 1 Hz. More than that, it should be emphasized that  $\chi''$  is considerably recognized only between  $T_A$  and  $T_C$ . At 600 Oe,  $\chi''$  is almost absent regardless of temperature and frequency, as shown in Fig. 4 (f). The existence of  $\chi''$  with the frequency region of 1 – 1000 Hz indicates that spin dynamics slows down to the time scale of 0.001 – 1 s only between  $T_A$  and  $T_C$  in low field. It is a clear evidence of emergence of the anomalous phase apart from a conventional ferromagnetic ordered state in  $\text{Co}_3\text{Sn}_2\text{S}_2$ .

### 3.3. Magnetic phase diagrams

Here we present the magnetic phase diagrams of  $\text{Co}_3\text{Sn}_2\text{S}_2$  based on the magnetization and AC susceptibility data described above. Figure 5(a) illustrate the  $H$ - $T$  phase diagram in the case of applied magnetic fields along the  $c$ -axis. In the phase diagram,  $T_C$  and  $T_A$  obtained from the FC magnetization and ZFC AC susceptibility are plotted.  $T_A$  is assigned by the hump anomaly in the FC magnetization and ZFC  $\chi'$  and  $T_C$  is assigned by the sharp peak anomaly in the FC magnetization, ZFC  $\chi'$  and  $\chi''$ . The  $HT$ -region surrounded by  $T_A$  and  $T_C$  is

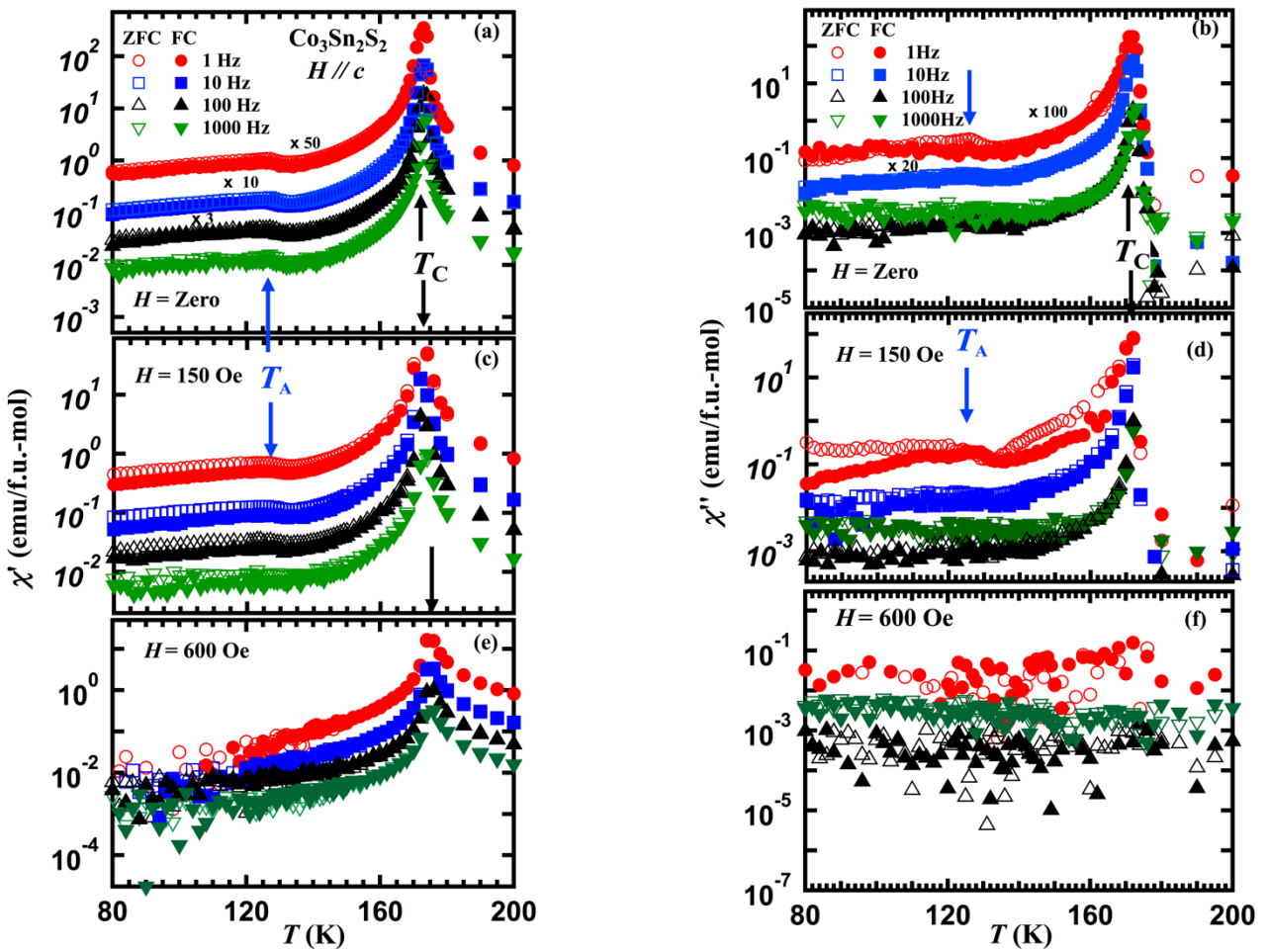
denoted as the A-phase. In Fig. 5 (a), the saturation field  $H_s$  where the magnetization collapses to the high-field-limit magnetization is also plotted. It should be noted that  $H_s(T)$  merges the high-field boundary of  $T_A(H)$ , which suggests the A-phase is characterized by a non-trivial spin texture before collinear ferromagnetic state is stabilized by magnetic field.

Figure 5 (b) illustrates the  $HT$  phase diagram in the case of applied magnetic field perpendicular to the  $c$ -axis. The A-phase boundary is not closed because the magnetization dose not saturate in this field direction due to the high magnetic anisotropy.

### 3.4. Relaxation phenomena and frequency dependence of $\chi'$ and $\chi''$ .

The existence of a non-zero  $\chi''$  in the A-phase, particularly around  $T_C$  and  $T_A$ , as indicated in sec. 3.2, implies that the spin dynamics slows down to the experimental window of  $f$ . To see the slow spin dynamics in the A-phase in detail, the frequency dependence of the AC susceptibility of  $\text{Co}_3\text{Sn}_2\text{S}_2$  is shown in details in Fig. 6 at temperatures below and in the A-phase.

The ZFC  $\chi'$  and  $\chi''$  at several temperatures under  $H = 150$  Oe are displayed in Figs. 6 (a) and



**Figure 4:** Thermal variation of ZFC and FC  $\chi'$  and  $\chi''$  of  $\text{Co}_3\text{Sn}_2\text{S}_2$  measured at different frequencies from 1 to 1000 Hz and for magnetic fields  $H$  of zero (a),(b), 150 Oe (c),(d), and 600 Oe (e),(f), applied along the  $c$ -axis. The arrows indicate  $T_C$  and  $T_A$  (see text). For clarity purpose, the data with frequencies of 1, 10 and 100 Hz have been shifted vertically with respect to the baseline by multiplying their data to the numbers indicated as in (a) and (b).



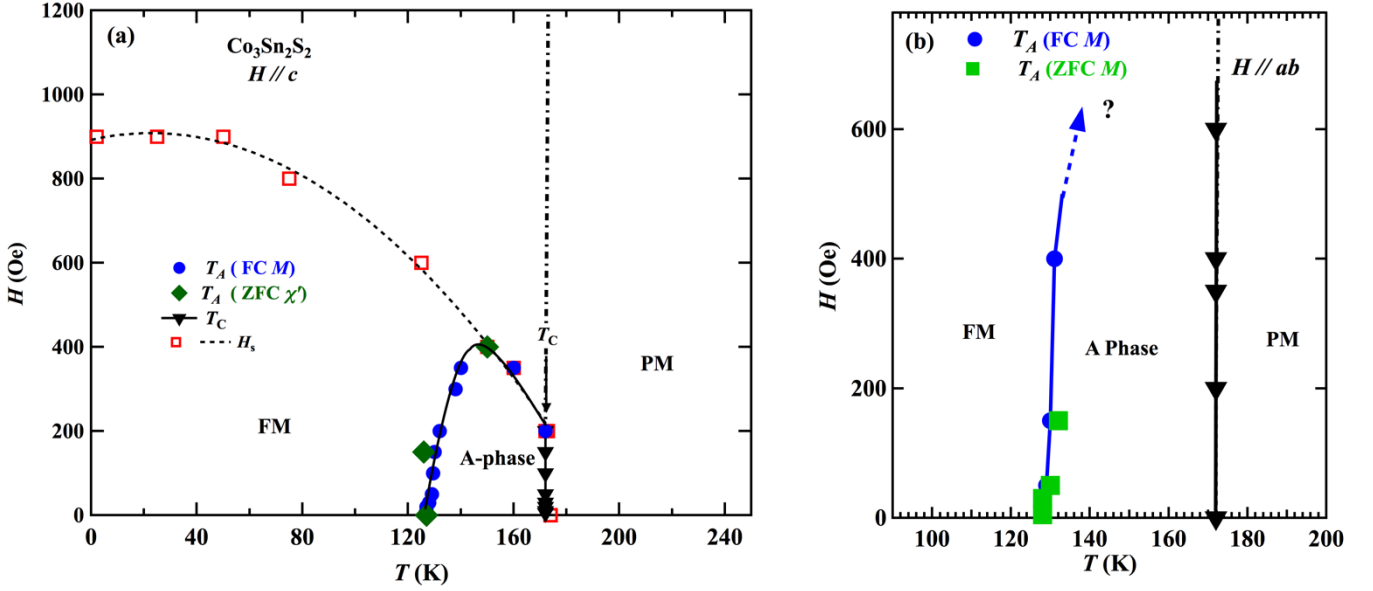


**Figure 5:** Magnetic  $H$ - $T$  phase diagrams of  $\text{Co}_3\text{Sn}_2\text{S}_2$  for fields applied (a) along and (b) perpendicular to the  $c$ -axis. Dashed and solid lines are for the eye guidance.

(b).  $\chi'$  below and around  $T_A$  are weakly frequency-dependent, and correspondingly,  $\chi''$  are almost absent. The increased value of  $\chi''$ , below  $T_A$ , at high  $f$  can be ascribed as an indication of  $f$ -dependence at higher  $f$ , that was found only in the MHz range in ferromagnetic materials<sup>31</sup>, or likely is an extrinsic effect due to eddy currents at low temperatures. While the boundary from the FM to A-phase at  $T_A$  is considered by the hump-like anomaly of  $\chi'$ , described in sec. 3.2, it is not detectable. The frequency dependence of  $\chi'$  and  $\chi''$  becomes more. The featureless  $\chi'$  and  $\chi''$  are seen until 135 K, where the minimum is found. At 160 K, deeper inside the A-phase,  $\chi'$  and  $\chi''$  exhibit pronounced frequency-dependence.  $\chi''$  strongly increases down to 0.5 Hz, indicating the longer time-scale of spin dynamics than 2 s at 160 K.

The frequency dependence of  $\chi'$  and  $\chi''$  becomes more pronounced with approaching to the high-temperature boundary between the A- and paramagnetic phases as shown in Figs. 6(c) and (d). It is clearly found that the time-scale of spin dynamics becomes shorter with  $T$ -increasing and exceeds the experimental frequency-window at 173 K, above  $T_C$ . The  $f$ -dependence of  $\chi'$  and  $\chi''$  at  $T_C$ , 172 K at  $H = 0.00$  Oe, for different magnetic fields is shown in Figs. 6(e) and (f). The frequency dependences of  $\chi'$

and  $\chi''$  at  $T_C$  do not change significantly, indicating weak variation of the time scale of spin dynamics with increasing of  $H$  at  $T_C$ . Both  $\chi'$  and  $\chi''$  are only suppressed with approaching the high field boundary of the A-phase,  $\sim 250$  Oe. Above this field, both  $\chi'$  and  $\chi''$  are very small and almost frequency-independent. It can be interpreted as that spins are fixed along the field-direction more and more and the number of slowly fluctuating spins is reduced by magnetic field.

To reveal an overview of the development of spin dynamics in the A-phase, phenomenological Cole-Cole formalism that includes a distribution of spin relaxation times<sup>32,33</sup> is employed. In the Cole-Cole analysis, the AC susceptibility is given by:

$$\chi(\omega) = \chi(\infty) + \frac{A_0}{1 + (i\omega\tau_0)^{1-\alpha}}, \quad (1)$$

with  $A_0 = \chi(0) - \chi(\infty)$ , where  $\chi(0)$  and  $\chi(\infty)$  are the isothermal and adiabatic susceptibilities,  $\omega = 2\pi f$  is the angular frequency and  $\alpha$  is a parameter that provides a measure of the width of the distribution of the relaxation time.  $\alpha = 0$  reverts Eq. (1) to the conventional Debye relaxation with a single relaxation time and  $\alpha = 1$  gives an infinite width of the distribution. The real and imaginary parts of the AC susceptibility can be extracted from Eq. (1) as<sup>32-34</sup>:

$$\chi'(\omega) = \chi(\infty) + \frac{A_0 [1 + (\omega\tau_0)^{1-\alpha} \sin(\pi\alpha/2)]}{1 + 2(\omega\tau_0)^{1-\alpha} \sin(\frac{\pi\alpha}{2}) + (\omega\tau_0)^{2(1-\alpha)}} \quad (2)$$

$$\chi''(\omega) = \frac{A_0 (\omega\tau_0)^{1-\alpha} \cos(\pi\alpha/2)}{1 + 2(\omega\tau_0)^{1-\alpha} \sin(\frac{\pi\alpha}{2}) + (\omega\tau_0)^{2(1-\alpha)}} \quad (3)$$

The fitting results to Eqs. (2), (3) just in the vicinity of  $T_C$  are shown as solid curves in Figs. 6(c), (e), (d) and (f). The fitting parameters are shown as functions of temperature at 150 Oe and as functions on the applied field at 172 K in the insets of Figs. 6(d) and (f), respectively. An estimated  $\alpha$  little varying at around 0.6 against  $T$  and  $H$  indicates a significant distribution of relaxation times, and its weak variation against  $T$  and  $H$ . On the other hand, the characteristic frequency,  $f_0 = 1/\tau_0$  varies. Especially,  $f_0$  drastically decreases with decreasing temperature at around  $T_C$ , i.e.  $f_0 \sim 25$  Hz, at 172 K, and  $f_0 \sim 0.1$  Hz at 171 K, and lower  $f_0$  is observed for  $T = 170$  K. The variation of  $f_0$  at  $T_C$  against  $H$  is more gentle, as seen in the inset of Fig. 6(f).

Actually it should be noted that an asymmetric bell-shaped  $f$ -dependence of  $\chi''$  shows

clear deviations from the Cole-Cole formalism at low frequency for  $T$ - and  $H$ -regions corresponding to the A-phase as seen in Figs. 6 (d) and (f). It indicates more complicated dynamics in the A-phase.

#### 4. Discussion

The magnetization and AC susceptibility indicate a zero- and low-field characteristic magnetic transitions to nontrivial spin state just below  $T_C$ . The magnetic relaxation process of characteristic relaxation times of several seconds at around borders of the anomalous A-phase and longer inside indicates a frozen phase. The slow spin dynamics in the A-phase can be initially ascribed to a glassy spin state<sup>35</sup>. However, the excluded disorder in our system and moreover the ferromagnetic order of fast relaxation of few microseconds below the anomalies transition temperatures,  $T_A$ , indicates the absence of a glassy state of spins. Given the arrangement of Co atoms of  $\text{Co}_3\text{Sn}_2\text{S}_2$  in kagomé sublattices in its 2D metallic layers, another spin state that results in these slow

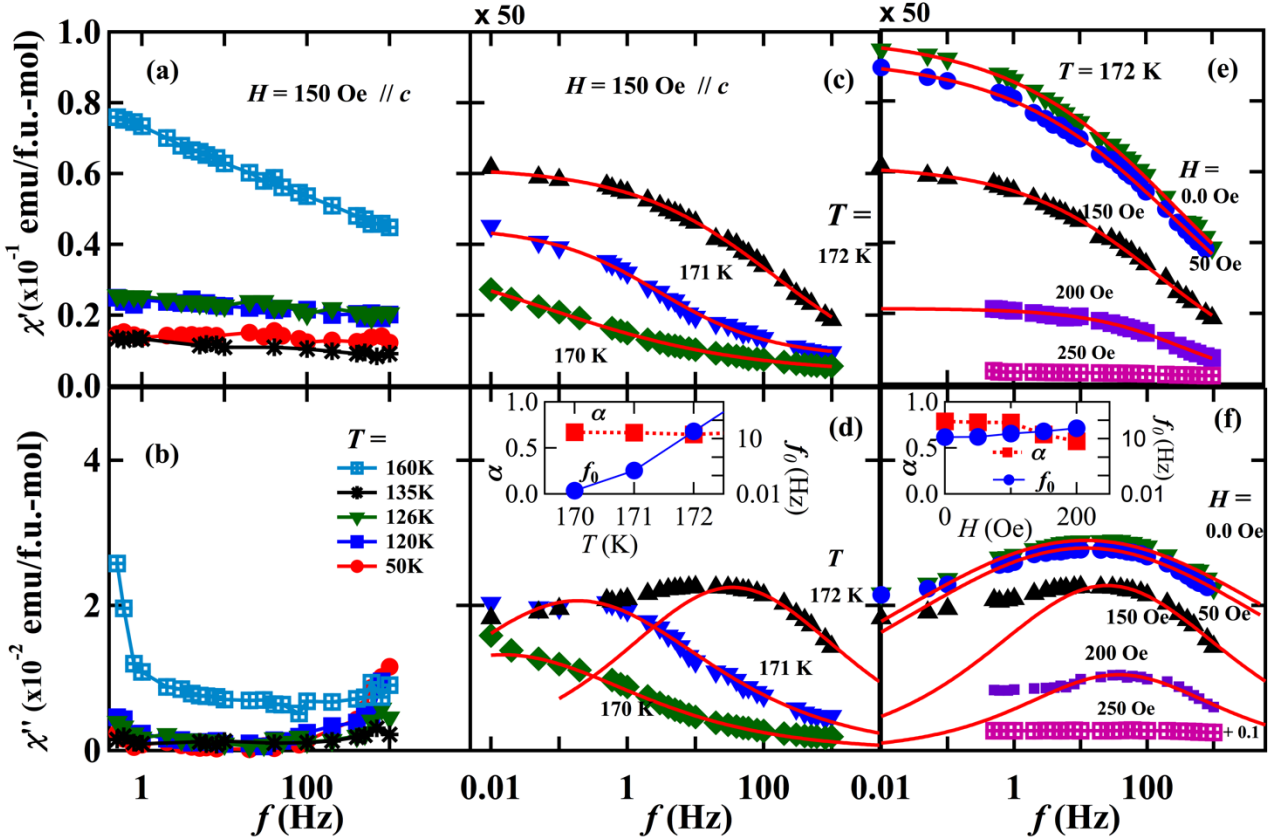


**Figure 6:** Frequency dependences of ZFC- $\chi'$  and  $\chi''$  of  $\text{Co}_3\text{Sn}_2\text{S}_2$  at  $T = 50 - 160$  K shown in (a), (b) and at 170-172 K (close to  $T_C$ ) shown in (c), (d), under a magnetic field of 150 Oe applied along the  $c$ -axis. (e) and (f) show ZFC- $\chi'$  and  $\chi''$  at  $T_C \sim 172$  K for different fields up to 250 Oe applied along the  $c$ -axis.

relaxation processes is that of large scale units such as magnetic skyrmions. The DM interaction in kagomé ferromagnets as well as the spin frustration exchanges that can be emerged by the enhanced fluctuations in the vicinity of  $T_C$ , as described in sec. 1, are possible mechanisms of a multi- $\mathbf{Q}$  spin state. Spin frustration is theoretically expected as a mechanism of magnetic skyrmions stabilization<sup>36</sup>.

Characteristic anomalous magnetic transitions just below  $T_C$  have been observed in B20 chiral magnets, FeGe<sup>15</sup>, MnSi<sup>37</sup>, Fe<sub>0.7</sub>Co<sub>0.3</sub>Si<sup>38</sup> and Cu<sub>2</sub>OSeO<sub>3</sub><sup>34,39</sup> at around the A-phase in these materials. The net magnetization as well as the AC susceptibility are minimal in the A-phase due to its non-coplanar spin structure at spots, i.e. skyrmions of antiparallel spins at the core and the peripheral and curled spins in between, in a ferromagnetic background. The quite stable state of magnetic skyrmions exhibits slow spin dynamics and the narrow temperature window of  $f$ -dependence of characteristic frequency,  $f_0$ , in the experiment frequency range at the A-phase borders have been previously observed in these skyrmion-hosting materials. The spin relaxation process exhibits a relaxation time distribution in the vicinity of  $T_C$  and has been described well by the Cole-Cole formalism<sup>34,38–40</sup>. The observation of asymmetrically distributed relaxation times inside the A-phase with experimental out-of-phase susceptibility,  $\chi''(f)$ , higher than that of the Cole-Cole formalism support the possible stable spin structure of magnetic skyrmions in Co<sub>3</sub>Sn<sub>2</sub>S<sub>2</sub> A-phase. Deviations of the  $\chi''(f)$  from the Cole-Cole formalism at low frequencies have been observed in (Fe,Co)Si<sup>38</sup>.

In contrast to a zero- and low-field stabilized spiral order, as a result of the balance between a strong ferromagnetic and a weaker DM interactions, in skyrmions-hosting chiral and polar magnets<sup>18,41</sup>, the A-phase in Co<sub>3</sub>Sn<sub>2</sub>S<sub>2</sub> is stabilized at zero field. This controversy may be ascribed to the spin frustration effects which are enhanced at low-fields by the thermal fluctuations very close to  $T_C$ .

Furthermore, an extended A-phase phase has recently been observed in centrosymmetric hexagonal magnets hosting biskyrmions<sup>42</sup>. Beyond the possible individual skyrmions stabilization by the

competing DM interaction, magnetic biskyrmions are stabilized by the dipolar interaction which possibly occurs in Co<sub>3</sub>Sn<sub>2</sub>S<sub>2</sub>. To address these expectations, further small-angle neutron scattering (SANS) experiments, spin-polarized scan tunneling microscopy (STM) or Lorentz TEM microscopy are needed to shed light on the bulk nature of the magnetic structures of Co<sub>3</sub>Sn<sub>2</sub>S<sub>2</sub>.

## 5. Conclusion

The precise measurement of the low-field magnetization process of Co<sub>3</sub>Sn<sub>2</sub>S<sub>2</sub> provides an approach to the  $H$ - $T$  phase diagram. Magnetic transitions at the borders of an anomalous pocket, A-phase, as indicated by the DC magnetization and the AC susceptibility were observed just below the magnetic order temperature,  $T_C$ . The disappearance of the anomalous transitions at higher fields suggests unconventional spin textures, probably of magnetic skyrmions, different from the ferromagnetic state in the A-phase. Frequency-distributed spin relaxation process of characteristic relaxation times of several seconds have been observed close to the A-phase boundary.

## Acknowledgement

M.A.K. would like to thank the Egyptian Ministry of Higher Education for financial support during his study in Kyoto University, Japan. This work was partly supported by Murata scientific foundation.

## References:

- <sup>1</sup> L. Balents, Nature **464**, 199 (2010).
- <sup>2</sup> H.T. Diep, editor, *Magnetic Systems with Competing Interactions: Frustrated Spin System* (World Scientific, Singapore, 1994).
- <sup>3</sup> Y. Taguchi, Y. Oohara, H. Yoshizawa, N. Nagaosa, and Y. Tokura, Science **291**, 2573 (2001).
- <sup>4</sup> Y. Machida, S. Nakatsuji, S. Onoda, T. Tayama, and T. Sakakibara, Nature **463**, 210 (2010).
- <sup>5</sup> D. Grohol, K. Matan, J.-H. Cho, S.-H. Lee, J.W. Lynn, D.G. Nocera, and Y.S. Lee, Nat. Mater. **4**, 323 (2005).
- <sup>6</sup> K. Ohgushi, S. Murakami, and N. Nagaosa, Phys. Rev. B **62**, R6065 (2000).
- <sup>7</sup> J.T. Chalker and J.F.G. Eastmond, Phys. Rev. B **46**, 14201 (1992).
- <sup>8</sup> M. Elhajal, B. Canals, and C. Lacroix, Phys. Rev. B **66**, 014422 (2002).
- <sup>9</sup> K. Matan, B.M. Bartlett, J.S. Helton, V. Sikolenko, S. Mat'aš, K. Prokeš, Y. Chen, J.W. Lynn, D. Grohol, T.J. Sato, M. Tokunaga, D.G. Nocera, and Y.S. Lee, Phys. Rev. B **83**, 214406 (2011).

- <sup>10</sup> I. Dzyaloshinsky, J. Phys. Chem. Solids **4**, 241 (1958).
- <sup>11</sup> T. Moriya, Phys. Rev. **120**, 91 (1960).
- <sup>12</sup> U.K. Rößler, A.N. Bogdanov, and C. Pfleiderer, Nature **442**, 797 (2006).
- <sup>13</sup> S. Mühlbauer, B. Binz, F. Jonietz, C. Pfleiderer, A. Rosch, A. Neubauer, R. Georgii, and P. Böni, Science **323**, 915 (2009).
- <sup>14</sup> W. Münzer, A. Neubauer, T. Adams, S. Mühlbauer, C. Franz, F. Jonietz, R. Georgii, P. Böni, B. Pedersen, M. Schmidt, A. Rosch, and C. Pfleiderer, Phys. Rev. B **81**, 041203 (2010).
- <sup>15</sup> X.Z. Yu, N. Kanazawa, Y. Onose, K. Kimoto, W.Z. Zhang, S. Ishiwata, Y. Matsui, and Y. Tokura, Nat. Mater. **10**, 106 (2011).
- <sup>16</sup> S. Seki, X.Z. Yu, S. Ishiwata, and Y. Tokura, Science **336**, 198 (2012).
- <sup>17</sup> Y. Tokunaga, X.Z. Yu, J.S. White, H.M. Rønnow, D. Morikawa, Y. Taguchi, and Y. Tokura, Nat. Commun. **6**, 7638 (2015).
- <sup>18</sup> I. Kézsmárki, S. Bordács, P. Milde, E. Neuber, L.M. Eng, J.S. White, H.M. Rønnow, C.D. Dewhurst, M. Mochizuki, K. Yanai, H. Nakamura, D. Ehlers, V. Tsurkan, and A. Loidl, Nat. Mater. **14**, 1116 (2015).
- <sup>19</sup> P. Ramdohr, Sitz. Berl. Akad. Wiss. Math.-Nat. Kl. VI **1**, (1949).
- <sup>20</sup> R. Weihrich, S.F. Matar, V. Eyert, F. Rau, M. Zabel, M. Andratschke, I. Anusca, and T. Bernert, Prog. Solid State Chem. **35**, 309 (2007).
- <sup>21</sup> R. Weihrich and I. Anusca, Z. Anorg. Allg. Chem. **632**, 335 (2006).
- <sup>22</sup> R. Weihrich, I. Anusca, and M. Zabel, Z. Anorg. Allg. Chem. **631**, 1463 (2005).
- <sup>23</sup> R. Weihrich, I. Anusca, and M. Zabel, Z. Anorg. Allg. Chem. **630**, 1767 (2004).
- <sup>24</sup> R. Weihrich and I. Anusca, Z. Anorg. Allg. Chem. **632**, 1531 (2006).
- <sup>25</sup> M. Holder, Y. Dedkov, A. Kade, H. Rosner, W. Schnelle, A. Leithe-Jasper, R. Weihrich, and S.L. Molodtsov, Phys. Rev. B **79**, 205116 (2009).
- <sup>26</sup> W. Schnelle, A. Leithe-Jasper, H. Rosner, F.M. Schappacher, R. Pöttgen, F. Pielhofer, and R. Weihrich, Phys. Rev. B **88**, 144404 (2013).
- <sup>27</sup> X. Lin, S.L. Bud'ko, and P.C. Canfield, Philos. Mag. **92**, 2436 (2012).
- <sup>28</sup> M.A. Kassem, Y. Tabata, T. Waki, and H. Nakamura, J. Phys. Soc. Jpn. **85**, 64706 (2016).
- <sup>29</sup> M.A. Kassem, Y. Tabata, T. Waki, and H. Nakamura, J. Cryst. Growth **426**, 208 (2015).
- <sup>30</sup> M.A. Kassem, Y. Tabata, T. Waki, and H. Nakamura, J. Solid State Chem. **233**, 8 (2016).
- <sup>31</sup> M. Balanda, Acta Phys. Pol. A **124**, 964 (2013).
- <sup>32</sup> K.S. Cole and R.H. Cole, J. Chem. Phys. **9**, 341 (1941).
- <sup>33</sup> C. Dekker, A.F.M. Arts, H.W. de Wijn, A.J. van Duynveldt, and J.A. Mydosh, Phys. Rev. B **40**, 11243 (1989).
- <sup>34</sup> F. Qian, H. Wilhelm, A. Aqeel, T.T.M. Palstra, A.J.E. Lefering, E.H. Brück, and C. Pappas, Phys. Rev. B **94**, 064418 (2016).
- <sup>35</sup> K. Binder and A.P. Young, Rev. Mod. Phys. **58**, 801 (1986).
- <sup>36</sup> T. Okubo, S. Chung, and H. Kawamura, Phys. Rev. Lett. **108**, 017206 (2012).
- <sup>37</sup> Y. Li, N. Kanazawa, X.Z. Yu, A. Tsukazaki, M. Kawasaki, M. Ichikawa, X.F. Jin, F. Kagawa, and Y. Tokura, Phys. Rev. Lett. **110**, 117202 (2013).
- <sup>38</sup> L.J. Bannenberg, A.J.E. Lefering, K. Kakerai, Y. Onose, Y. Endoh, Y. Tokura, and C. Pappas, Phys. Rev. B **94**, 134433 (2016).
- <sup>39</sup> I. Levatić, V. Šurija, H. Berger, and I. Živković, Phys. Rev. B **90**, 224412 (2014).
- <sup>40</sup> A. Bauer and C. Pfleiderer, Phys. Rev. B **85**, 1 (2012).
- <sup>41</sup> N. Nagaosa and Y. Tokura, Nat. Nanotechnol. **8**, 899 (2013).
- <sup>42</sup> W. Wang, Y. Zhang, G. Xu, L. Peng, B. Ding, Y. Wang, Z. Hou, X. Zhang, X. Li, E. Liu, S. Wang, J. Cai, F. Wang, J. Li, F. Hu, G. Wu, B. Shen, and X.X. Zhang, Adv. Mater. **28**, 6887 (2016).

---

\* E-mail: [kassem.ahmed.82s@st.kyoto-u.ac.jp](mailto:kassem.ahmed.82s@st.kyoto-u.ac.jp) or [makassem@aun.edu.eg](mailto:makassem@aun.edu.eg)

† Permanent Address: Department of Physics, Assiut University, Assiut 71515, Egypt